Influences of Atlantic Warm Pool on Western Hemisphere Summer Rainfall and Atlantic Hurricanes

Chunzai Wang[1]
David B. Enfield[1]
Sang-ki Lee[2]
Christopher W. Landsea[3]

[1] Physical Oceanography Division
NOAA Atlantic Oceanographic and Meteorological Laboratory
Miami, Florida

[2] Cooperative Institute for Marine and Atmospheric Studies
University of Miami
Miami, Florida

[3] Hurricane Research Division
NOAA Atlantic Oceanographic and Meteorological Laboratory
Miami, Florida

Submitted to *Journal of Climate*

January 2005

Corresponding author address: Dr. Chunzai Wang, NOAA/AOML/PHOD, 4301 Rickenbacker Causeway, Miami, FL 33149. E-mail: Chunzai.Wang@noaa.gov.

Abstract

Both tropical Pacific and Atlantic climate phenomena affect rainfall variations in the Western Hemisphere and these impacts are seasonally dependent. As Pacific ENSO matures in the boreal winter, its correlations with rainfall from North to South Americas and in the tropical Atlantic are maximized. As the ENSO-dominated effects fade in the boreal spring, the tropical Atlantic meridional gradient variability, defined by the SST anomaly difference between the tropical North Atlantic and South Atlantic, emerges as the leading influence on rainfall distributions in the tropical Atlantic and surrounding land areas. During the boreal summer, the large Atlantic warm pool and warm tropical North Atlantic are associated with increased rainfall over the Caribbean, Mexico, the eastern subtropical Atlantic, and the southeast Pacific, and decreased rainfall in northwest US and Canada, and eastern South America. In particular, summer rainfall in the Caribbean and southeastern Mexico is mainly related to the size of the Atlantic warm pool. The large Atlantic warm pool, associated with a decrease in sea level pressure and an increase in atmospheric convection and cloudiness, corresponds to a weak vertical wind shear and thus increases Atlantic hurricane activity. The Atlantic Niño, a counterpart of the Pacific El Niño, shows wet conditions in the entire equatorial Atlantic, the Guinean region, northern South America, Mexico, and the subtropical North Atlantic and dry conditions over South America between 5°S and 25°S and north of the equatorial eastern Pacific.

1. Introduction

The El Niño-Southern Oscillation (ENSO) affects precipitation variations over the globe (e.g., Ropelewski and Halpert 1987, 1989; Diaz et al. 2001). When ENSO's sea surface temperature (SST) anomalies in the equatorial eastern Pacific reach their maximum during the boreal winter, the heat source of the western Pacific warm pool shifts eastward and alters atmospheric convective activity leading to ENSO teleconnections on a global scale. Figure 1a shows Western Hemisphere (WH) map of the correlation of December-January-February (DJF) rainfall anomalies with the DJF Nino3 (5°S-5°N, 150°W-90°W) SST anomalies (see Section 2 for detail in data and calculation). A major feature for ENSO-related winter rainfall is an oppositely signed rainfall correlation pattern over a long latitudinal band of the northern and southern Caribbean, with positive correlation from the subtropical North Atlantic to the western United States (US) and negative correlation from northern South America to north of the equatorial Atlantic (as well as over northeast Brazil). A transition zone separating the positive and negative rainfall correlations is located around 18-20°N. Figure 1a also shows boreal winter rainfall increase over South America south of 20°S and over a small region in the tropical South Atlantic.

During the boreal summer, however, either in the development/decay phases of El Niño or neutral condition, equatorial eastern Pacific SST anomalies are relatively weak and ENSO teleconnections are different from those in the boreal winter (Alexander et al. 2004). Figure 1b displays the correlation map of August-September-October (ASO) rainfall anomalies with the ASO Nino3 SST anomalies. During ASO, the northern band of positive rainfall correlation disappears. In fact, Figure 1b agrees with some studies that a negative correlation exists over the Caribbean and Central America (e.g., Enfield and Alfaro 1999; Giannini et al. 2000; Diaz et al.

2001; Chen and Taylor 2002; Taylor et al. 2002; Spence et al. 2004) and in northern South America and the western equatorial Atlantic (Fig. 1b).

Tropical Atlantic variability also affects WH rainfall (e.g., Moura and Shukla 1981; Folland et al. 1986; Enfield 1996; Giannini et al. 2000; Taylor et al. 2002; Spence et al. 2004). One of important tropical Atlantic climate phenomena is the tropical Atlantic meridional gradient variability that is defined by the SST anomaly difference between the tropical North Atlantic (TNA; 6°N-22°N, 60°W-15°W) and the tropical South Atlantic (TSA; 0°-20°S, 30°W-10°E). This meridional SST gradient variability, correlated with north-south displacements of the Atlantic intertropical convergence zone (ITCZ), has maximum variance during the boreal spring. Its impact on spring (March-April-May, MAM) rainfall in the WH is shown in Fig. 1c. The rainfall correlation patterns display an antisymmetric distribution over the TNA and TSA. Moura and Shukla (1981) showed an antisymmetric distribution of gridded SST anomalies correlated with northeast Brazil rainfall although the TNA and TSA SST anomalies are mostly independent (e.g., Houghton and Tourre 1992; Enfield and Mayer 1997; Mehta 1998; Enfield et al. 1999; Dommenget and Latif 2000; Melice and Servain 2003). The significant rainfall correlations extend the surrounding land regions, with negative correlation in northeast Brazil and positive correlation for northwest Africa and northern part of South America. Enfield (1996) discusses the relationships of inter-American rainfall (all seasons) with the TNA, the TSA, and the Atlantic ITCZ, and Enfield et al. (1999) have explained how the SST anomaly dipole pattern occurs in spite of the fact that the TNA and TSA SST anomalies are not correlated.

Other tropical Atlantic climate phenomena include the Atlantic Niño and Atlantic warm pool. The Atlantic Niño is an interannual phenomenon centered in the equatorial Atlantic, similar to but weaker and more frequent than the Pacific El Niño (e.g., Zebiak 1993; Carton and

Huang 1994). The Atlantic Niño SST anomalies reach their peaks during the boreal summer and the size of the Atlantic warm pool is also maximized in the boreal summer. Unlike the Pacific El Niño and the tropical Atlantic meridional gradient variability, rainfall distributions associated with the Atlantic Niño and the Atlantic warm pool are relatively unknown. Given the fact that the dominant effects of the Pacific El Niño and the tropical Atlantic meridional gradient variability on rainfall are in the winter and spring, respectively, it is not surprising that the Atlantic Niño and the Atlantic warm pool play some roles in summer rainfall distributions in their surrounding regions. In this paper we report observational evidence of direct relationships between WH rainfall and the Atlantic Niño and Atlantic warm pool during the boreal summer when their variations are maximum.

Interannual and longer timescale Atlantic hurricane activity has been linked to a variety of features including the Pacific El Niñ/La Niña, Caribbean sea level pressure (SLP) and tropospheric vertical wind shear, the stratospheric Quasi-Biennial Oscillation, African West Sahel rainfall, and Atlantic SST (e.g., Gray 1984; Landsea et al. 1999). Because tropical cyclones extract energy from the warm tropical oceans and release the heat in its upper tropospheric outflow to fuel the storm's development, warmer SSTs can lead to more intense hurricanes. A few studies (Raper 1992, Shapiro and Goldenberg 1998, and Saunders and Harris 1997) have linked both concurrent and preceding SST anomalies in the Atlantic to local tropical cyclone activity. Enfield and Mestas-Nunez (1999) and Mestas-Nunez and Enfield (1999) showed that tropical North Atlantic SST variability is tied to simultaneous alterations in the high latitudes of the North Atlantic in a mode that resides primarily at the multidecadal timescale (50-80 years). Gray (1990), Gray et al. (1997) and Landsea et al. (1999) made links of these long-term SST variations to Atlantic tropical cyclone activity, primarily with the "major" hurricanes—those with maximum sustained surface winds of at least 50 m/s. Goldenberg et al. (2001) concluded that beginning in 1995, the North Atlantic switched back to the warm phase after two and a half decades of the cool phase. Along with the switch in SSTs, the Atlantic region saw a resurgence of major hurricane activity. It is expected that variations in the size of the Atlantic warm pool might also be related to Atlantic hurricane activity; however, the relationship has not been documented in the literature yet. This paper thus will also explore the relationship between the Atlantic warm pool and Atlantic hurricanes.

The paper is organized as follows. Section 2 discusses the data sets and methods that are used in this paper. Section 3 briefly describes the Atlantic warm pool and the Atlantic Niño. Section 4 shows influences of the eastern Pacific warm pool, the Atlantic warm pool, and the Atlantic Niño on the WH rainfall variability. Section 5 documents the relationship between the Atlantic warm pool and Atlantic hurricanes. Finally, Section 6 discusses possible explanations of rainfall variability and Atlantic hurricanes, and provides a summary.

2. Data and methods

Many data sets are used in this study. The first is an improved extended reconstructed SST dataset on a 2° latitude by 2° longitude grid beginning January 1854 (Smith and Reynolds 2004), but here we only analyze monthly SST from January 1950 to December 2003. The second data set is the product of the CPC (Climate Prediction Center) Merged Analysis of Precipitation (CMAP) on a 2.5° latitude by 2.5° longitude grid from January 1979 to April 2004 that includes monthly precipitation by merging rain gauge data and five kinds of satellite estimates (Xie and Arkin 1997). The third data set is the NCEP-NCAR reanalysis (we use velocity potential and divergent wind at 200-mb and 850-mb) from Janunary 1950 to December 2003 on a 2.5° latitude by 2.5° longitude grid (Kalnay et al. 1996).

The fourth data set is the hurricane data from the official U.S. National Hurricane Center archives (Jarvinen et al. 1984) for the North Atlantic basin, comprised of the North Atlantic Ocean, Gulf of Mexico and Caribbean Sea. Hurricanes are defined as having maximum sustained (1 min) surface (10 m) winds of at least 33 m/s somewhere in its circulation. The database extends back to 1851 (Landsea et al. 2004), but only data from 1950 through 2003 are utilized here. The period of the second half of the 20th Century is considered to be generally complete and reliable in the frequency and intensity of tropical cyclones in the database (Neumann et al. 1999), though short-lived, weak systems may have been missed before the era of geostationary satellite coverage began in the mid-1960s. This may cause a slight (estimated to be less than one hurricane every two years) underreporting bias in the period of 1950 to 1965.

Our analyses include the calculation of different indices, composite averages, and cross-correlations between the seasonally stratified anomaly indices and contemporaneous CMAP rainfall anomalies and Atlantic hurricanes. Contingency table analysis is also used to examine the relationship between the Atlantic warm pool and hurricane frequency. In correlation calculations, the significance of the correlations is determined by the method of Sciremammano (1979), which accounts for serial correlation in the data (Davis 1976).

3. Atlantic warm pool and Atlantic Niño

The Western Hemisphere warm pool (WHWP), the region covered by water warmer than 28.5°C, undergoes large annual and interannual variations (Wang and Enfield 2001, 2003; hereafter WE0103). Unlike the Eastern Hemisphere warm pool in the western Pacific (e.g., Webster and Lukas 1992), which straddles the equator, the WHWP is entirely north of the equator. At various stages of development, the WHWP is comprised of the eastern North Pacific (ENP) west of Central America, the Intra-Americas Sea (IAS), i.e., the Gulf of Mexico and the Caribbean, and the western TNA. Figure 2a shows the June-July-August (JJA) WHWP area anomaly index of WE0103. From 1950-2003, the five largest WHWPs (1958, 1969, 1983, 1987, 1998) have occurred during the boreal summers following the Pacific El Niño events (Fig. 2b). However, four other El Niño events (1966, 1973, 1977, 1992) are not associated with large WHWPs. Enfield et al. (2005) discuss factors that control the development of large WHWPs and why this happens.

The WHWP includes two ocean regions: (1) the ENP west of Central America and (2) the Gulf of Mexico, the Caribbean, and the western TNA. The two warm water regions are separated by the Central America landmass. Figure 2c shows the component area index for the ENP portion of the WHWP. In all of the five large WHWPs following El Niño peaks, the ENP has a large area. This is an expected result since the ENP is close to the ENSO region of maximum variance and is directly related to ENSO variability.

In this paper, since we mainly focus on non-ENSO factors that influence WH rainfall and Atlantic hurricanes, we will consider the Atlantic portion of the WHWP (the Atlantic warm pool). We note the two facts: (1) the annual precipitation of central America and the Caribbean exhibits a bimodal distribution with maxima during the early summer of June and the late summer of September-October (e.g., Magana et al. 1999; Taylor et al. 2002) and (2) the Atlantic warm pool peaks around September and disappears in the boreal winter (WE0103). Therefore, our analysis of rainfall will address variability during both the early summer of May-June-July (MJJ) and the later summer of August-September-October (ASO). The boreal summer is the season for which ENSO-related teleconnections are weakest—especially in the Northern Hemisphere—and the need for predictability from other sources is greatest. Figure 3a and b show the MJJ and ASO percentage area anomalies of the Atlantic warm pool, based on the area of SST warmer than 28.5°C normalized by the MJJ and ASO climatological warm pool area, respectively. In four (1958, 1969, 1987, 1998) of five largest WHWPs (Fig. 2a), the Atlantic warm pool is also large. For year 1983 (a large WHWP), the Atlantic warm pool is normal in both the early and late summer. In comparison of Figs. 3a and b, the Atlantic warm pool in MJJ is more affected by the Pacific El Niño than ASO. This is to be expected because some of El Niño effects are weakening fast.

In ASO, we identify a warm pool 25% larger (smaller) than the climatological area as a large (small) warm pool; otherwise, warm pool is classified as normal or neutral. From 1950-2003, there are 14 large warm pools (1952, 1958, 1969, 1980, 1987, 1990, 1995, 1997, 1998, 1999, 2000, 2001, 2002, 2003) and 15 small warm pools (1950, 1965, 1967, 1971, 1972, 1974, 1975, 1976, 1977, 1982, 1984, 1985, 1986, 1992, 1994). Based on well-documented ENSO events, no Pacific El Niño occurs in the preceding boreal winter for 9 of the 14 years of large warm pools (1952, 1980, 1990, 1995, 1997, 1999, 2000, 2001, 2002). Among the 15 small warm pools, there are 10 cases (1950, 1967, 1972, 1975, 1977, 1982, 1984, 1985, 1992, 1994) in which the preceding winter does not show a La Niña condition in the Pacific.

In Fig. 4, we composite the 14 large warm pools and the 15 small warm pools comparing them with the ASO climatological mean. The large warm pool is almost three times larger than that of the small one (their areas are 8.0×10^6 km^2 and 2.8×10^6 km^2, respectively). In summary, the variability of the Atlantic warm pool is large, and although Pacific ENSO teleconnections are clearly influential on the Atlantic side, about two thirds of the overall warm pool variability (both large and small warm pools) there appears unrelated to ENSO during the late summer.

As reviewed recently by Wang et al. (2004), a common feature of all three tropical oceans is for the Bjerknes' positive ocean-atmosphere feedback to exist in all ocean basins. In the tropical Atlantic, the Bjerknes' feedback mechanism results in the Atlantic Niño (Zebiak 1993) that is similar to the Pacific El Niño. The Atlantic Niños resemble their Pacific counterparts in that they involve the disappearance of the cold tongue of water along the equator (during the boreal summer), a surge of warm tropical water eastward and then southward along the southern coast of Africa, an anomalous reversal of direction of the equatorial trade winds, and shifts of atmospheric convection towards the anomalous warm water in the east. However, they are weaker and more frequent than the Pacific El Niños. The spatial and temporal variability of the Atlantic Niño can be found in many studies (e.g., Zebiak 1993; Carton and Huang 1994; Latif and Grotzner 2000; Wang 2002a). In contrast to Pacific ENSO influence on TNA variability, some observational analyses (e.g., Zebiak 1993; Enfield and Mayer 1997) show that the correlation between the equatorial Atlantic and eastern Pacific SST anomalies is generally insignificant, suggesting that the Atlantic Niño is largely independent of Pacific ENSO. The 1984 Atlantic Niño event is one exception that may result from the intense 1982-83 El Niño (Delecluse et al. 1994). One reason that the Atlantic Niño appears to be less affected by Pacific ENSO than the TNA may be related to the different seasons to which they are phase-locked. The Atlantic Niño appears primarily in the boreal summer, which makes it difficult for Pacific ENSO to have a direct influence on it since Pacific ENSO peaks in the boreal winter.

4. Rainfall variability

Before we focus on the influence of the Atlantic Ocean on WH rainfall variability, we first examine the impact of the eastern north Pacific (ENP) warm pool on rainfall variability.

a. ENP warm pool

As shown in WE0103, the ENP warm pool starts to develop in the early boreal spring and it is well developed by May. Figure 5a shows the correlation map of the April-May-June (AMJ) rainfall anomalies with the AMJ ENP warm pool area index. Positive correlation is found over the equatorial eastern Pacific and the tropical and subtropical North Atlantic, whereas negative correlation is located in the region of the eastern Pacific ITCZ and from the equatorial eastern South America to the tropical South Atlantic. This correlation pattern is very similar to that of the AMJ rainfall anomalies with the AMJ Nino3 SST anomalies, as shown in Fig. 5b. This is not a surprising result since the ENP frequently has significant SST anomalies that persist well into the following spring of an El Niño event. In other words, interannual variation of the ENP warm pool is directly related to El Niño events. However, Fig. 5 does not necessarily mean that Pacific El Niño is directly responsible for the rainfall correlations in the Atlantic sector. In the boreal spring, the TNA is being warmed through the El Niño connected atmospheric process described by Enfield et al. (2005). The TNA is correlated with meridional displacements of the ITCZ. Therefore, the Atlantic rainfall correlations can be explained as being associated with El Niño only by proxy through the TNA SST and the Atlantic ITCZ (e.g., Enfield 1996; Taylor et al. 2002).

b. Atlantic warm pool

We first examine the relationship between rainfall and the Atlantic warm pool during the early summer (MJJ). The contemporaneous correlation of the MJJ rainfall anomalies with the MJJ Atlantic warm pool area index is shown in Fig. 6a. The MJJ warm pool is correlated with rainfall over some small regions. The most interesting results may be negative correlation near Texas and positive correlation over western US. The ENSO-influenced rainfall during MJJ is displayed in Fig. 6b. Figure 6b does not show a significant correlation near Texas and over western US. This suggests that rainfall variability in these two regions during MJJ is related to the Atlantic warm pool.

The correlation map of the ASO rainfall anomalies with the ASO Atlantic warm pool area index is shown in Fig. 7a. Significant positive correlation is found over the Caribbean, Mexico and Central America, the eastern tropical and subtropical North Atlantic, and the southeast Pacific, while negative correlation is located over the northwest US and Great Plains regions, and eastern South America. As showed in Fig. 1b and in the studies of Giannini et al. (2000), Diaz et al. (2001), and Chen and Taylor (2002), the Pacific El Niño-related rainfall correlation during the boreal summer is negative over the Caribbean, the Pacific side of Central America, and the southeast Pacific. The ENSO-related rainfall correlation is positive over northwest US and Canada (Fig. 1b). That is, the signs of rainfall correlation with the Atlantic warm pool in these regions are opposite to those for Nino3 SST anomalies. Therefore, we can infer that summer wet and dry conditions in these regions have a direct association with Atlantic SST rather than Pacific El Niño. This is consistent with the result presented in Section 3 in that two thirds of ASO Atlantic warm pool events occur without preceding winter Pacific ENSO events. However, the Atlantic warm pool is associated with dry conditions in northeastern South America and wet conditions west of the Mediterranean, just as Nino3 is. A warm TNA (large warm pool) is associated with a northward displacement of the Atlantic ITCZ, which is consistent with less rainfall in northeast Brazil, suggesting that these anomalies may be more directly linked to the warm pool and/or TNA than to Pacific El Niño. However, based solely on the signs of the correlations we cannot infer conclusively which ocean is linked directly to summer rainfall of those regions.

Based on our definition of the Atlantic warm pool (SST $\geq$ 28.5°C), for most of the time the Atlantic warm pool is geographically different from the TNA. However, there is some overlap between the warm pool and TNA domains, but only when the eastern limits of the large warm pool extend east of the 60°W meridian. As showed in WE0103, the size of the Atlantic warm pool is correlated with the TNA SST anomalies. Figure 7b shows the correlation between the ASO rainfall anomalies and the ASO TNA SST anomalies. As expected, the correlation patterns in Figs. 7a and b are similar. However, the significant positive correlation over the Caribbean and southeastern Mexico region in Fig. 7a does not appear in Fig. 7b, while the positive correlation off west Africa extends west and covers a larger area. This suggests that rainfall variation in the Caribbean and southeastern Mexico region is mainly related to the Atlantic warm pool, with a large (small) warm pool having more (less) rainfall in the boreal late summer.

The negative correlation over the Great Plains region (Fig. 7) makes sense from a moisture transport perspective. Much of the summer moisture that precipitates over the Great Plains is exported from the warm pool to the north (Bosilovich and Schubert 2001, 2002). If more (less) moisture precipitates over the warm pool, it seems plausible that less (more) would be available for transport into the Great Plains region. The possible reasons for the negative rainfall correlations over the northwestern US are less obvious, however.

The positive rainfall correlation in the southeast Pacific is interesting. It is unlikely that this feature is directly related to ENSO because Fig. 1b shows either insignificant or negative correlation with ENSO in this region. The possible linkage between the Atlantic warm pool (the TNA) and the southeast Pacific may be the regional Hadley circulation. Figure 8 shows the composites of the 200-mb velocity potential and divergent wind anomalies for the large and small warm pools. Large warm pools are associated with a strong regional Hadley cell emanating from south of the warm pool into the southeast Pacific where anomalous convergence is located (Fig. 8a). The converse occurs for small warm pools (Fig. 8b). Considering that the southeast Pacific is the region of anticyclone with climatological subsidence there (e.g., Wang and Enfield 2003), large (small) warm pools strengthen (weaken) subsidence over the southeast Pacific. In the subsidence region of the southeast Pacific, the surface winds evaporate water vapor from the ocean, but the atmospheric inversion prevents the moist air from rising to significant elevations. A thin layer of stratus clouds form at the base of that inversion. Recently, Y. Wang et al. (2004) show a light precipitation, usually named drizzle, under the stratus cloud deck over the southeast Pacific. This is consistent with the results shown in this paper. We note that rainfall is relatively low under the stratus deck and this is a region where only satellite data are available, hence this region deserves closer study. However, our analysis (Figs. 7-8) does show a relationship among the Atlantic warm pool, and rainfall and the Hadley circulation over the southeast Pacific.

c. Atlantic Niño

The warm Atlantic Niño events reach their maximum strength in the boreal summer, with manifestations focused primarily near the equator (e.g., Zebiak 1993; Carton and Huang 1994;

Latif and Grotzner 2000; Wang 2002a). During a warm phase, trade winds in the equatorial western Atlantic are weak and SST is high in the equatorial eastern Atlantic. The reverse occurs during a cold phase. Figure 9 shows the correlation map of the June-July-August (JJA) rainfall anomalies with the JJA Atl3 (4°S-4°N, 20°W-0°) SST anomalies. The Atlantic Niño is associated with more rainfall over the entire equatorial Atlantic and the Guinean region. The remote impacts include wet conditions over northern South America, Mexico, and the subtropical North Atlantic, and dry conditions over South America between 5°S and 25°S and north of the equatorial eastern Pacific. The Pacific ENSO and the TNA show either opposite signs of correlations or no significant correlations in these regions during the boreal summer (Fig. 1b and Fig. 7b), suggesting that summer rainfall over these regions is related to the equatorial Atlantic SST anomalies.

An interesting feature of Fig. 9 is an opposite correlation pattern between the equatorial Atlantic and north of the equatorial Pacific. This raises a question about the relationship between the Atlantic Niño and the Pacific El Niño. As stated in the introduction, some observational analyses show no statistical evidence for linkage between the equatorial Atlantic and Pacific SST anomalies (e.g., Zebiak 1993; Enfield and Mayer 1997). Our calculation shows that the correlation between the JJA Atl3 SST anomalies and the JJA Nino3 SST anomalies is 0.01. This may again suggest that the Atlantic Niño is directly involved in the rainfall patterns of Fig. 9. The opposite correlation pattern between the Atlantic and Pacific may be due to that the rainfall is responding to the zonal SST gradient between the equatorial Atlantic and Pacific that results from anomalous extremes in either the basin alone or from dipole configurations (Enfield and Alfaro 1999; Spence et al. 2004). This is in a manner analogous to the tropical Atlantic meridional gradient variability that is associated with an antisymmetric rainfall correlation between the TNA and TSA (e.g., Moura and Shukla 1981; Fig. 1c), however, the TNA and TSA SST anomalies are mostly independent.

5. Atlantic hurricanes

The rainfall correlation maps of Fig. 7 show that the Atlantic warm pool and TNA have a significant positive correlation off West Africa extending westward and covering the tropical eastern north Atlantic. This is the region where easterly waves moving offshore of the Sahel region frequently become hurricanes during August and September, which then propagate westward toward the Caribbean and North America. Increased rainfall is indicative of greater tropospheric instability, which favors cyclogenesis (Gray 1968). Knaff (1997) has shown that when the Caribbean and western TNA are warm, the troposphere is less stable, rainfall in the region is greater, and hurricane activity increases. Our results support the notion that large warm pools are associated with greater Atlantic hurricane activity.

Figure 10a compares the total numbers of Atlantic hurricanes with the ASO Atlantic warm pool area anomaly index. Our calculation shows that the correlation coefficient of the Atlantic warm pool area with the Atlantic hurricanes is 0.33 which is above the 95% significance level. This correlation is very encouraging and important, in comparison with the correlation of –0.39 between the ASO Nino3 SST anomalies and Atlantic hurricanes (also see Landsea et al. 1999). The Atlantic warm pool is related to hurricane activity because the SST partly determines the maximum potential development of the storms. Within the warm pool, the temperatures required for development extend to greater depth than elsewhere, thus reducing the tendency of a storm to diminish that potential by mixing cool water into the upper warm layer (Bender and Ginis 2000; Shay et al. 2000). Hence, the size of the warm pool is important because it affects the area (fetch) over which the intensity and heat content required for sustained development are available.

Gray (1968 and 1979) showed that a major inhibiting factor for tropical cyclone and hurricane is tropospheric vertical wind shear. The vertical wind shear (VWS) between the upper troposphere (200-mb) and the lower troposphere (850-mb) can be calculated as:

$$VWS = \sqrt{(U_{200} - U_{850})^2 + (V_{200} - V_{850})^2}\ .$$

The VWS in the IAS region during ASO is shown in Figs. 10b and c, in comparison with the Atlantic warm pool area index and the total numbers of the Atlantic hurricanes. The calculation shows that the VWS is significantly correlated with the Atlantic warm pool area index (-0.36) and the total numbers of Atlantic hurricanes (-0.47). WE0103 show that the IAS SST anomalies are correlated with the IAS SLP and cloudiness anomalies. Combining these results, the physical mechanism that links the warm pool and Atlantic hurricane activity can thus be described as follows. Warm water causes a decrease in SLP anomalies which result in an anomalous increase in deep convective activity (also see Knaff 1997) and atmospheric cloudiness. This is associated with a weak vertical wind shear (Figs. 10b and c) that can strengthen the tropical cyclone by helping the organization of deep convection and thus increases Atlantic hurricane activity. The weaker vertical wind shear means that weaker upper level (200-mb) westerly and weaker low level (850-mb) easterly. The weakened low level easterly may feedback to the ocean for warming SSTs.

The Atlantic hurricanes can be grouped into subsets based on the region of their formation, intensity, and season. We stratify them into seven groups: (1) forming in the IAS (including the Gulf of Mexico and the Caribbean Sea), (2) forming in the TNA (60°W-0, 0-30°N), (3) all categories 1-2 (based on the Saffir-Simpson hurricane scale), (4) all categories 3-5 (major hurricanes), (5) forming in early season (June-July, JJ), (6) forming in mid season (August-September, AS; also called Cape Verde), and (7) forming in late season (October-November, ON). The official Atlantic hurricane season is from June 1 to November 30 and it is traditionally divided into JJ, AS, and ON. Table 1 compares the mean hurricane count per year of large warm pools with that of small warm pools for these seven hurricane groups and the total Atlantic hurricanes. Statistical significance of differences of the mean is assessed by applying a Student t-test. Hurricanes forming in the TNA, major hurricanes, hurricanes forming in the mid and late seasons, and all Atlantic hurricanes show significantly different means for large and small warm pools (Table 1). Among these significant groups, the two largest differences for small and large warm pools are those of major hurricanes and those forming in the TNA. As an example, Fig. 11 contrasts major hurricane tracks of 14 years of large warm pools and of 15 years of small warm pools.

The linear correlations of hurricanes with the JJ, AS, and ON warm pool indices are calculated, as shown in Table 2. From this table, several points can be mentioned. First, the linear correlations of the Atlantic warm pool with hurricanes forming in the IAS are very low. This may reflect the warm water distribution of the Atlantic warm pool. It is generally considered that tropical waters warmer than 26-27°C favor the development of large-scale convection and are necessary for hurricane development (Gray 1968). Because during the hurricane season the IAS has climatological SSTs above the convective threshold (26-27°C) throughout the hurricane season, a larger or smaller warm pool will not greatly affect SSTs in that region of formation. Thus, we do not expect the warm pool to have a strong effect on hurricanes forming in the IAS. Second, the correlations of the Atlantic warm pool with hurricanes forming in the early season (JJ) are also very low. This is consistent with the fact that few hurricanes form in the early season and those that do are usually formed in the IAS. Third, the Atlantic warm pool shows significant correlations (above the 95% significant level) with the hurricanes forming in the TNA region and in the mid season. Finally, the fact that the Atlantic warm pool is significantly correlated with all Atlantic hurricanes testifies to the strength of the relationship in those groups where it is significant, as well as to their numerical dominance in the season totals.

Another statistical method that can be applied to detect the association between the Atlantic warm pool and hurricanes is the contingency table. Table 3 shows a 3-by-3 contingency table for all Atlantic hurricanes and the Atlantic warm pool. All hurricanes are divided into terciles, with the upper (lower) tercile representing active (inactive) hurricane years (18 years each). Similarly, large (small) warm pool years are ones within the top (bottom) third when ranked by warm pool size. The joint years are then found and filled for each cell. The χ^2 test of significance for this table is above the 95% significance level. For the 54 years from 1950 to 2003, only 2 of the 18 years with small warm pools are active hurricane years, while 11 of the 18 years with large warm pools are active years. Similarly, 4 of the 18 years with large warm pools are inactive years and 8 of the 18 years with small warm pools are inactive years. Again, it shows that large (small) Atlantic warm pools favor (disfavor) Atlantic hurricanes.

6. Discussion and summary

a. ENSO-related rainfall

The largest climate signal in the instrumental record is ENSO, which extends its reach globally through atmospheric teleconnections. As the Pacific El Niño matures in the boreal winter, its associated rainfall anomalies show an oppositely signed pattern over the northern and southern Caribbean: a wet condition along a long latitudinal band from the subtropical Atlantic Ocean to western US and a dry condition from northern South America to north of the equatorial Atlantic Ocean. A transition zone separating the wet and dry bands is located around 18°-20°N. Although this ENSO-related rainfall distribution over the WH is relatively well known, to our knowledge we do not see that previous studies have explained why the opposite sign of rainfall pattern can happen.

The analyses of the NCEP-NCAR reanalysis show that as the El Niño warming culminates near the end of the calendar, an alteration of the tropical direct atmospheric circulation occurs. The schematic diagram, summarizing observations of the anomalous boreal winter Walker/Hadley circulation over the eastern Pacific and Atlantic, is shown in Fig. 12 (from Wang 2002a and b). Associated with the Pacific El Niño, the air anomalously ascends in the equatorial eastern Pacific, diverges eastward in the upper troposphere, and then converges and descends over northern South America and the western equatorial Atlantic. The anomalous descending motion can explain why northern South America and the equatorial Atlantic are dry during the winter of typical El Niño years. At the same time, Fig. 12 shows an anomalous Hadley circulation with ascending motion in the subtropical region. The anomalous ascending motion over the western Atlantic could be attributed to a weaker subtropical high that allows a more frequent southward penetration of winter frontal systems that has wet condition over north of the Caribbean. Over west of the subtropical Atlantic, the positive rainfall correlation may be due to a southward-displaced storm track (Compo and Sardeshmukh 2004) downstream of major circulation changes in the North Pacific. During the boreal winter of La Niña year, a reversal of the anomalous atmospheric Walker and Hadley circulations occurs. This provides a possible explanation for the opposite sign pattern of the ENSO-related rainfall over the northern and southern Caribbean as shown in Fig. 1a.

b. Tropical Atlantic meridional gradient variability and rainfall

As Pacific ENSO decays after the boreal winter, other climate phenomena may emerge to influence WH rainfall variability. The tropical Atlantic meridional gradient variability, defined by the SST anomaly difference between the TNA and TSA, correlates with an antisymmetric rainfall distribution over the TNA and TSA during the boreal spring (Fig. 1c). The NCEP-NCAR reanalysis field shows that the meridional SST gradient variability is observed to correspond to an atmospheric meridional circulation cell (Wang 2002a). When the meridional SST anomaly gradient is positive (negative), the air rises over the TNA (TSA), flows toward the TSA (TNA) aloft, converges in the upper troposphere to feed the strong subsidence and lower tropospheric divergence in the TSA (TNA), then crosses the equator toward the TNA (TSA) in the lower troposphere. This meridional circulation cell is consistent with the rainfall correlation of Fig. 1c. The positive (negative) meridional SST anomaly gradient corresponds to anomalous ascent (descent) over the TNA and anomalous descent (ascent) over the TSA that result in more (less) and less (more) rainfall, respectively.

c. Atlantic warm pool, Atlantic Niño, and rainfall

Since the ENP warm pool is close to the ENSO region of maximum variance and is directly related to ENSO variability, its rainfall correlation is very similar to that of ENSO. However, the Atlantic warm pool is different. If a warm pool 25% larger (smaller) than its climatological size is defined as a large (small) warm pool, two thirds of Atlantic warm pool events occur without preceding winter Pacific ENSO events. Thus, the Atlantic warm pool displays some rainfall influences that are different from ENSO. Although the Atlantic warm pool is geographically different from the TNA for most of the time, the size of the warm pool is correlated with the TNA SST anomalies (WE0103). As a result, their rainfall correlations display some similarities and dissimilarities. We should keep in mind that the atmosphere responds to the total, rather than to the anomalous SST. Thus, in the region of the warm pool (as in the western Pacific warm pool), a small SST anomaly change can produce a relatively large atmospheric response. From this point of view, the Atlantic warm pool may play a more active role for atmospheric response.

During the early summer of MJJ, the Atlantic warm pool shows a negative correlation near Texas and a positive correlation over western US. As the size of the Atlantic warm pool maximizes during the late summer of ASO, it induces more rainfall over the Caribbean and southeastern Mexico (the TNA SST anomalies do not show significant correlations in these regions). This rainfall relationship is consistent with oceanic and atmospheric conditions observed over the warm pool region. WE0103 showed that the warm SST anomalies in the Atlantic warm pool are associated with a decrease in SLP anomalies and an anomalous increase in atmospheric convection and cloudiness. Years with a large warm pool have lower SLP and vertical shear, greater moist instability over the region of the Atlantic warm pool, and a weakened tropical upper tropospheric trough (Knaff 1997). These conditions lead to generally great and contemporaneous summer rainfall over the region surrounding the warm pool and an increase in tropical cyclone activity.

The Atlantic warm pool also shows a positive rainfall correlation over the southeast Pacific where the drizzle under the stratus cloud deck usually appears. Our analysis (Fig. 8) shows that a possible link between the Atlantic warm pool and the southeast Pacific is the regional Hadley circulation. Large (small) Atlantic warm pools strengthen (weaken) the summer Hadley circulation that emanates from the region of the warm pool into the southeast Pacific. This will change the subsidence over the southeast Pacific and thus the stratus cloud and rainfall. That is, the stratus deck in the southeast Pacific responds to externally imposed variations of the Atlantic warm pool in subsidence via the regional Hadley circulation.

The Atlantic Niño's atmospheric response is similar to that of the Pacific El Niño. It is not surprising to see positive rainfall correlation in the equatorial Atlantic since previous studies have showed that the Atlantic Niño is associated with equatorial Atlantic positive diabatic heating (Ruiz-Barradas et al. 2000) and anomalous ascending vertical motion in the middle troposphere (Wang 2002a). However, it is not clear how the Atlantic Niño remotely affects rainfall variations. It may be like Pacific ENSO in that heat source in the equatorial Atlantic associated with warm SST anomalies changes atmospheric circulation patterns that affect rainfall over remote regions. Numerical models are needed to investigate this topic. The Atlantic Niño's rainfall correlation shows an opposite sign between the equatorial Atlantic and eastern Pacific (Fig. 9). However, the Atl3 SST anomalies are uncorrelated with the Nino3 SST anomalies. This may be analogous to the north-south dipole in the tropical Atlantic (TNA vs. TSA). It is the east-west SST gradient between the two oceans that induces an anomaly in the east-to-west flow of air across northern South American and a corresponding direct circulation aloft between the two oceans, both of which can lead to a dichotomy in rainfall between the two oceans.

Finally, the current rainfall prediction in the WH largely depends on the Pacific ENSO condition. The present study shows that, in addition to Pacific ENSO, other climate phenomena like the tropical Atlantic meridional gradient variability, the Atlantic warm pool, the Atlantic

Niño, and the Atlantic multidecadal oscillation (Enfield et al. 2001) also affect WH rainfall distributions. Future rainfall forecasts should consider these additional factors.

d. Atlantic warm pool and Atlantic hurricanes

Our statistical analysis shows that large Atlantic warm pools are associated with greater Atlantic hurricane activity. The relationship may be discussed from two points of view: (1) hurricanes' continued development and/or intensification and (2) formation of Atlantic hurricanes. From the point of view of the hurricanes' development/intensification, the Atlantic warm pool is related to hurricane activity because the upper ocean temperature partly determines the maximum potential development of hurricanes and because warm pool characteristics are correlated with changes in vertical shear, known to affect development (e.g., Knaff 1997). Within the warm pool, the temperatures required for development extend to greater depth than elsewhere, thus reducing the tendency of a storm to diminish that potential by mixing cool water into the upper warm layer. Hence, the size of the warm pool is important because it affects the area over which the intensity and heat content required for sustained development are available. As a storm passes over the warm pool, it will be intensified or further developed. The calculations show that warm water corresponds to a decrease in SLP anomalies and an increase in deep convective activity and atmospheric cloudiness. This is associated with a weak vertical wind shear that can strengthen the tropical cyclone by helping the organization of deep convection and thus increases Atlantic hurricane activity.

The Atlantic warm pool may also relate to Atlantic hurricane activity through hurricanes' formation region. Our rainfall correlation maps show that the Atlantic warm pool and TNA have a significant positive correlation off West Africa extending westward and covering the tropical eastern north Atlantic. This is the region where easterly waves frequently become hurricanes, which then propagate westward toward the Caribbean and North America. Increased rainfall in this region is indicative of greater atmospheric instability, which favors cyclogenesis and thus is associated with greater Atlantic hurricane activity. However, a further study is needed to investigate physical mechanisms regarding the relationship among the Atlantic warm pool, the TNA, rainfall off West Africa and formation of Atlantic hurricanes.

Acknowledgments. This work was supported by a grant from National Oceanic and Atmospheric Administration (NOAA) Office of Global Programs and by the base funding of NOAA Atlantic Oceanographic and Meteorological Laboratory (AOML).

References

Alexander, M. A., N.-C. Lau, and J. D. Scott, 2004: Broadening the atmospheric bridge paradigm: ENSO teleconnections to the tropical west Pacific-Indian Oceans over the seasonal cycle and to the North Pacific in summer. In *Earth's Climate: The Ocean-Atmosphere Interaction*, edited by C. Wang, S.-P. Xie, and J. A. Carton, AGU Geophysical Monograph Series 147, 85-104.

Bender, M. A., and I. Ginis, 2000: Real-case simulations of hurricane-ocean interaction using a high-resolution coupled model: Effects on hurricane intensity. *Mon. Wea. Rev.*, **128**, 917-946.

Bosilovich, M. G., and S. D. Schubert, 2001: Precipitation recycling in the GEOS-1 data assimilation system over the central United States. *J. Hydrometeor.,* **2,** 26–35.

Bosilovich, M. G., and S. D. Schubert, 2002: Water vapor tracers as diagnostics of the regional hydrologic cycle. *J. Hydrometeor.*, **3**, 149-165.

Carton, J.A., and B. Huang, 1994: Warm events in the tropical Atlantic. *J. Phys. Oceanogr.*, **24**, 888-903.

Chen, A.A., and M.A. Taylor, 2002: Investigating the link between early season Caribbean rainfall and the El Niño+1 year. *Inter. J. of Climat.*, **22**, 87–106.

Compo, G. P. and P. D. Sardeshmukh, 2004: Storm Track predictability on seasonal and decadal scales. *J. Climate*, **17**, 3701-3720.

Davis, R. E., 1976: Predictability of sea surface temperature and sea level pressure anomalies over the North Pacific Ocean. *J. Phys. Oceanogr.*, **6**, 249-266.

Delecluse, P., J. Servain, C. Levy, K. Arpe, and L. Bengtsson, 1994: On the connection between the 1984 Atlantic warm event and the 1982-83 ENSO. *Tellus*, **46A**, 448-464.

Diaz, H.F., M.P. Hoerling, and J.K. Eischeid, 2001: ENSO Variability, Teleconnections and Climate Change. *Inter. J. of Climat.*, **21**, 1845–1862.

Dommenget, D., and M. Latif, 2000: Interannual to decadal variability in the tropical Atlantic. *J. Climate,* **13**, 777-792.

Enfield, D.B., 1996: Relationships of inter-American rainfall to tropical Atlantic and Pacific SST variability. *Geophys. Res. Lett.*, **23**, 3305-3308.

Enfield, D.B., and D.A. Mayer, 1997: Tropical Atlantic sea surface temperature variability and its relation to El Niño-Southern Oscillation. *J. Geophys. Res.*, **102**, 929-945.

Enfield, D.B., and E.J. Alfaro, 1999: The Dependence of Caribbean Rainfall on the Interaction of the Tropical Atlantic and Pacific Oceans. *J. Climate*, **12** (7), 2093-2103.

Enfield, D.B., A.M. Mestas-Nuñez, D.A. Mayer, and L. Cid-Serrano, 1999: How ubiquitous is the dipole relationship in tropical Atlantic sea surface temperatures? *J. Geophys. Res.*, **104**, 7841-7848.

Enfield, D.B., A.M. Mestas-Nunez, and P.J. Trimble, 2001: The Atlantic Multidecadal Oscillation and its relationship to rainfall and river flows in the continental US. *Geophys. Res. Lett.*, **28**, 2077-2080.

Enfield, D. B., S.-K. Lee, and C. Wang, 2005: How are large Western Hemisphere warm pools formed? To be submitted.

Folland, C.K., T.N. Palmer, and D.E. Parker, 1986: Sahel rainfall and worldwide sea temperatures, 1901-1985. *Nature*, **320**, 602-607.

Giannini, A., Y. Kushnir, and M.A. Cane, 2000: Interannual variability of Caribbean rainfall, ENSO and the Atlantic Ocean. *J. Climate*, **13**, 297-311.

Goldenberg, S.B., C.W. Landsea, A.M. Mestas-Nuñez, and W.M. Gray, 2001: The recent increase in Atlantic hurricane activity: Causes and implications. *Science,* **293,** 474-479.

Gray, W. M., 1968: Global view of the origions of tropical disturbances and storms. *Mon. Wea. Rev.*, **96**, 669-700.

Gray, W. M., 1979: Hurricanes: Their formation, structure, and likely role in the tropical circulation. Meteorology Over the Tropical Oceans, D. B. Shaw, Ed., Roy. Meteor. Soc., 155-218.

Gray, W. M., 1984: Atlantic seasonal hurricane frequency: Part I: El Niño and 30 mb quasi-biennial oscillation influences. *Mon. Wea. Rev.*, **112**, 1649-1668.

Gray, W. M., 1990: Strong association between West African rainfall and US landfall of intense hurricanes. *Science*, **249**, 1251-1256.

Gray, W. M., J. D. Sheaffer, and C. W. Landsea, 1997: Climate trends associated with multidecadal variability of Atlantic hurricane activity. Hurricanes, Climate and Socioeconomic Impacts, Edited by H. F. Diaz and R. S. Pulwarty, Springer, Berlin, 15-53.

Houghton, R.W., and Y.M. Tourre, 1992: Characteristics of low-frequency sea surface temperature fluctuations in the tropical Atlantic. *J. Climate*, **5**, 765-771.

Jarvinen, B. R., C. J. Neumann, and M. A. S. Davis, 1984: A tropical cyclone data tape for the North Atlantic Basin, 1886-1983: Contents, limitations, and uses. NOAA Technical Memorandum NWS NHC 22, Coral Gables, Florida, 21 pp.

Kalnay, E., and Co-authors, 1996: The NCEP/NCAR 40-year reanalysis project. *Bull. Am. Meteorol. Soc*., **77**, 437-471.

Knaff, J.A., 1997: Implications of summertime sea level pressure anomalies in the tropical Atlantic region. *J. Climate*, **10**, 789-804.

Landsea, C. W., R. A. Pielke, A. M. Mestas-Nunez, and J. A. Knaff, 1999: Atlantic basin hurricanes: Indices of climatic changes. *Climatic Change*, **42**, 89-129.

Landsea, C. W., C. Anderson, N. Charles, G. Clark, J. Dunion, J. Fernandez-Partagas, P. Hungerford, C. Neumann, and M. Zimmer, 2004: The Atlantic hurricane database re-analysis project: Documentation for the 1851-1910 alterations and additions to the HURDAT database. In *Hurricanes and Typhoons: Past, Present and Future*, R. J. Murname and K.-B. Liu, Eds., Columbia University Press, 177-221.

Latif, M., and A. Grotzner, 2000: The equatorial Atlantic oscillation and its response to ENSO. *Clim. Dyn.*, **16**, 213-218.

Magaña, V., J. A. Amador, and S. Medina, 1999: The midsummer drought over Mexico and central America. *J. Climate*, **12**, 1577-1588.

Mehta, V.M., 1998: Variability of the tropical ocean surface temperatures at decadal multidecadal timescales. Part I: The Atlantic Ocean. *J. Climate*, **11**, 2351-2375.

Melice, J.-L., and J. Servain, 2003: The tropical Atlantic meridional SST gradient index and its relationships with the SOI, NAO and Southern Ocean. *Clim. Dyn.*, **20**, 447-464.

Moura, A.D., and J. Shukla, 1981: On the dynamics of droughts in northeast Brazil: Observations, theory and numerical experiments with a general circulation model. *J. Atmos. Sci.*, **38**, 2653-2675.

Neumann, C. J., B. R. Jarvinen, C. J. McAdie, and G. R. Hammer, 1999: Tropical Cyclones of the North Atlantic Ocean, 1871-1999. NOAA/NWS/NESDIS, Historical Climatology Series 6-2, 206 pp.

Raper, S., 1992: Observational data on the relationships between climate change and the frequency and magnitude of severe tropical storms. In *Climate and sea level change: Observations, projections and implications*., R. A. Warrick, E. M. Barrow, and T. M. L. Wigley (Eds.). Cambridge University Press, 192-212.

Ruiz-Barradas, A., J. A. Carton, and S. Nigam, 2000: Structure of interannual-to-decadal climate variability in the tropical Atlantic sector. *J. Climate*, **13,** 3285-3297.

Ropelewski, C. F. and M. S. Halpert, 1987: Global and regional precipitation patterns associated with the El Nino/Southern Oscillation. *Mon. Wea. Rev*., **115**, 1606-1626.

Ropelewski, C. F. and M. S. Halpert, 1989: Precipitation patterns associated with the high index phase of the Southern Oscillation. *J. Climate*, **2**, 268-284.

Saunders, M. A., and A. R. Harris, 1997: Statistical evidence links exceptional 1995 Atlantic hurricane season to record sea warming. *Geo. Res. Lett*., **24**, 1255-1258.

Sciremammano, F., 1979: A suggestion for the presentation of correlations and their significance levels. *J. Phys. Oceanogr*, **9**, 1273-1276.

Shapiro, L. J., and S. B. Goldenberg, 1998: Atlantic sea surface temperatures and tropical cyclone formation. *J. Climate*, **11**, 578-590.

Shay, L. K., G. J. Goni, and P. G. Black, 2000: Effects of a warm oceanic feature on Hurricane Opal. *Mon. Wea. Rev*., **128**, 1366-1383.

Smith, T.M., and R.W. Reynolds, 2004: Improved Extended Reconstruction of SST (1854-1997). *J. Climate*, **17**, 2466-2477.

Spence, J.M., M.A. Taylor, and A. Chen, 2004: The effect of concurrent sea-surface temperature anomalies in the tropical Pacific and Atlantic on Caribbean rainfall. *Int. J. Climatol*., **24**, 1531-1541.

Taylor, M. A., D. B. Enfield, and A. A. Chen, 2002: Influence of the tropical Atlantic versus the tropical Pacific on Caribbean rainfall. *J. Geophys. Res*., **107** (C9), 3127, doi:10.1029/ 2001JC001097.

Wang, C., and D.B. Enfield, 2001: The tropical Western Hemisphere warm pool. *Geophys. Res. Lett*., **28**, 1635-1638.

Wang, C., 2002a: Atlantic climate variability and its associated atmospheric circulation cells. *J. Climate*, **15**, 1516-1536.

Wang, C., 2002b: ENSO and atmospheric circulation cells. *CLIVAR Exchanges*, **7**, 9-11.

Wang, C., and D. B. Enfield, 2003: A further study of the tropical Western Hemisphere warm pool. *J. Climate,* **16**, 1476-1493.

Wang, C., S.-P. Xie, and J. A. Carton, 2004: A global survey of ocean-atmosphere interaction and climate variability. In *Earth's Climate: The Ocean-Atmosphere Interaction*, edited by C. Wang et al., AGU Geophysical Monograph Series 147, 1-19.

Wang, Y. , S.-P. Xie, H. Xu, and B. Wang, 2004: Regional model simulations of marine boundary-layer clouds over the Southeast Pacific off South America. Part I: Control experiment. *Mon. Wea. Rev.,* **132** (1), 274–296.

Webster, P. J., and R. Lukas, 1992: The Tropical Ocean/Global Atmosphere Coupled Ocean-atmosphere Response Experiment (COARE). *Bull. Amer. Meteor. Soc.*, **73**, 1377-1416.

Xie, P., and P.A. Arkin, 1997: Global precipitation: A 17-year monthly analysis based on gauge observations, satellite estimates, and numerical model outputs. *Bull. Am. Meteorol. Soc.*, **78**, 2539-2558.

Zebiak, S. E., 1993: Air-sea interaction in the equatorial Atlantic region. *J. Climate*, **6**, 1567-1586.

Figure Captions

Figure 1. (a) Correlation of December-January-February (DJF) rainfall anomalies with the DJF Nino3 SST anomalies, (b) Correlation of August-September-October (ASO) rainfall anomalies with the ASO Nino3 SST anomalies, and (c) Correlation of March-April-May (MAM) rainfall anomalies with the MAM SST anomaly difference between the tropical North Atlantic (TNA) and tropical South Atlantic (TSA). The 90% and 95% significant levels are 0.33 and 0.39, respectively. The shadings represent correlation larger than 0.33 (dark for positive and light dark for negative).

Figure 2. (a) June-July-August (JJA) Atlantic warm pool area anomaly index (%), (b) December-January-February (DJF) Nino3 SST anomalies, and (c) April-May-June (AMJ) eastern North Pacific (ENP) warm pool area anomaly index (%). The warm pool indices are calculated as the anomalies of the area of SST warmer than 28.5°C divided by the climatological (JJA and AMJ, respectively) warm pool area.

Figure 3. (a) May-June-July (MJJ) Atlantic warm pool area anomaly index (%) and (b) August-September-October (ASO) Atlantic warm pool area anomaly index (%). The indices are calculated as the anomalies of the area of SST warmer than 28.5°C divided by the climatological (MJJ and ASO, respectively) warm pool area.

Figure 4. SST composites of (a) large Atlantic warm pools and (b) small Atlantic warm pools during August-September-October (ASO). The dark contour represents ASO climatological SST warmer than 28.5°C.

Figure 5. (a) Correlation of April-May-June (AMJ) rainfall anomalies with the AMJ eastern North Pacific (ENP) warm pool index, and (b) Correlation of AMJ rainfall anomalies with the AMJ Nino3 SST anomalies. The 90% and 95% significant levels are 0.33 and 0.39, respectively. The shadings represent correlation larger than 0.33 (dark for positive and light dark for negative).

Figure 6. (a) Correlation of May-June-July (MJJ) rainfall anomalies with the MJJ Atlantic warm pool index, and (b) Correlation of MJJ rainfall anomalies with the MJJ Nino3 SST anomalies. The 90% and 95% significant levels are 0.33 and 0.39, respectively. The shadings represent correlation larger than 0.33 (dark for positive and light dark for negative).

Figure 7. (a) Correlation of August-September-October (ASO) rainfall anomalies with the ASO Atlantic warm pool index, and (b) Correlation of ASO rainfall anomalies with the ASO SST anomalies in the tropical North Atlantic (TNA; 6°N-22°N, 60°W-15°W). The 90% and 95% significant levels are 0.33 and 0.39, respectively. The shadings represent correlation larger than 0.33 (dark for positive and light dark for negative).

Figure 8. Composites of the 200-mb velocity potential and divergent wind anomalies during August-September-October (ASO) for (a) large Atlantic warm pools and (b) small Atlantic warm pools.

Figure 9. Correlation of June-July-August (JJA) rainfall anomalies with the Atl3 (4°S-4°N, 20°W-0°) SST anomalies. The 90% and 95% significant levels are 0.33 and 0.39, respectively. The shadings represent correlation larger than 0.33 (dark for positive and light dark for negative).

Figure 10. (a) August-September-October (ASO) Atlantic warm pool area anomalies and the total number of Atlantic hurricanes, and (b) ASO Atlantic warm pool area anomalies and the vertical wind shear between the upper (200-mb) and lower (850-mb) troposphere in the IAS region (85°W-50°W, 10°N-25°N) during ASO, and (c) the ASO IAS vertical wind shear and the total number of Atlantic hurricanes. The R represents correlation coefficient at zero lag.

Figure 11. Atlantic major hurricane tracks for (a) 14 years of large Atlantic warm pools and (b) 15 years of small Atlantic warm pools.

Figure 12. Schematic diagram showing linkage of the Pacific El Niño with northern South America/equatorial Atlantic, the tropical North Atlantic (TNA), and the Western Hemisphere

warm pool (WHWP) by the anomalous Walker and Hadley circulations (from Wang 2002a and b). The anomalous Walker and Hadley circulations are drawn, based on the data analyzed from the NCEP-NCAR reanalysis field.

Table 1. Comparison of the mean hurricane number per year for large and small Atlantic warm pools. A warm pool 25% larger (smaller) than the climatological area is identified as a large (small) warm pool (see Section 3). Hurricanes are classified as (1) forming in the IAS, (2) forming in the TNA, (3) categories 1-2, (4) categories 3-5, (5) forming in early season (June-July), (6) forming in middle season (August-September), and (7) forming in late season (October-November). Differences significant above the 95% level are given in bold.

Hurricane Class	Large Warm Pool	Small Warm Pool	Change in Percent (%)	Significance Level (%)
Form in IAS	1.8	1.3	38%	76.8%
Form in TNA	**3.9**	**2.1**	**86%**	**99.9%**
All categories 1-2	4.6	3.5	31%	94.3%
All categories 3-5	**2.9**	**1.6**	**81%**	**99.8%**
Form in early season	0.6	0.3	100%	64.0%
Form in mid season	**4.9**	**3.5**	**40%**	**98.9%**
Form in late season	**2.0**	**1.2**	**67%**	**95.6%**
All hurricanes	**7.5**	**5.1**	**47%**	**99.9%**

Table 2. Linear correlation coefficients (R) and significant level (Sig in %) for eight hurricane classes (rows) versus the June-July (JJ), August-September (AS), and October-November (ON) Atlantic warm pool (WP) area indices. Hurricanes are classified as (1) forming in the IAS, (2) forming in the TNA, (3) categories 1-2, (4) categories 3-5, (5) forming in early season (JJ), (6) forming in middle season (AS), and (7) forming in late season (ON). The correlation above the 95% significant level is given in bold.

Hurricane Class	R (Sig) with JJ warm pool index	R (Sig) with AS warm pool index	R (Sig) with ON warm pool index
Form in IAS	0.14 (68.3%)	0.14 (69.0%)	0.00 (0.8%)
Form in TNA	**0.30 (97.4%)**	**0.32 (98.3%)**	**0.34 (98.9%)**
All categories 1-2	0.25 (93.1%)	0.24 (92.5%)	0.23 (91.0%)
All categories 3-5	0.21 (87.3%)	0.26 (94.3%)	0.17 (78.9%)
Form in early season	-0.09 (46.3%)	0.03 (14.4%)	0.06 (30.8%)
Form in mid season	**0.34 (98.8%)**	**0.29 (96.4%)**	**0.29 (96.5%)**
Form in late season	0.19 (82.1%)	0.24 (92.0%)	0.08 (45.9%)
All hurricanes	**0.33 (98.4%)**	**0.36 (99.2%)**	**0.29 (96.7%)**

Table 3. The contingency table for all Atlantic hurricanes versus the AS (August-September) Atlantic warm pool. The χ^2 value is 10.7 and its significance level is 97.0%.

	Inactive	Neutral	Active	Total
Small warm pool	8	8	2	18
Neutral warm pool	6	7	5	18
Large warm pool	4	3	11	18
Total	18	18	18	54

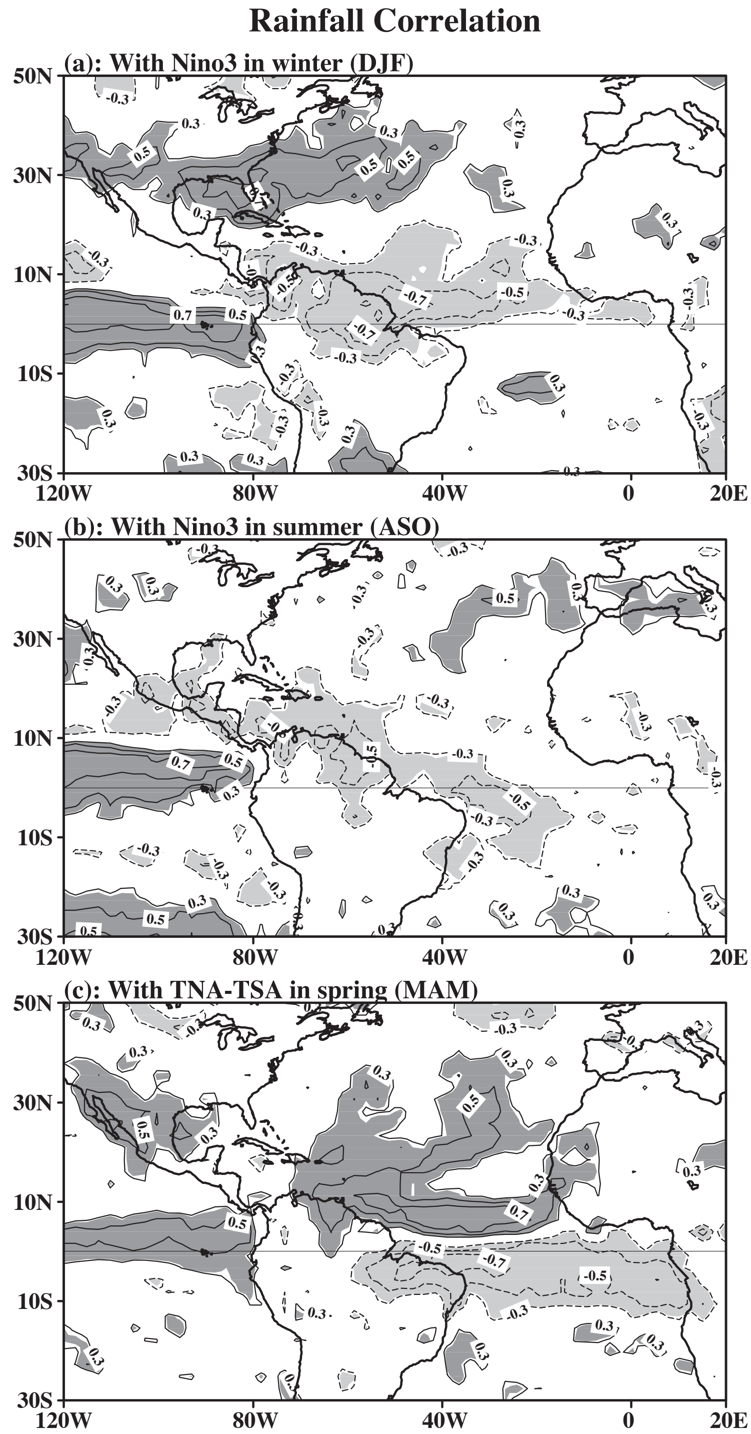

Figure 1. (a) Correlation of December-January-February (DJF) rainfall anomalies with the DJF Nino3 SST anomalies, (b) Correlation of August-September-October (ASO) rainfall anomalies with the ASO Nino3 SST anomalies, and (c) Correlation of March-April-May (MAM) rainfall anomalies with the MAM SST anomaly difference between the tropical North Atlantic (TNA) and tropical South Atlantic (TSA). The 90% and 95% significant levels are 0.33 and 0.39, respectively. The shadings represent correlation larger than 0.33 (dark for positive and light dark for negative).

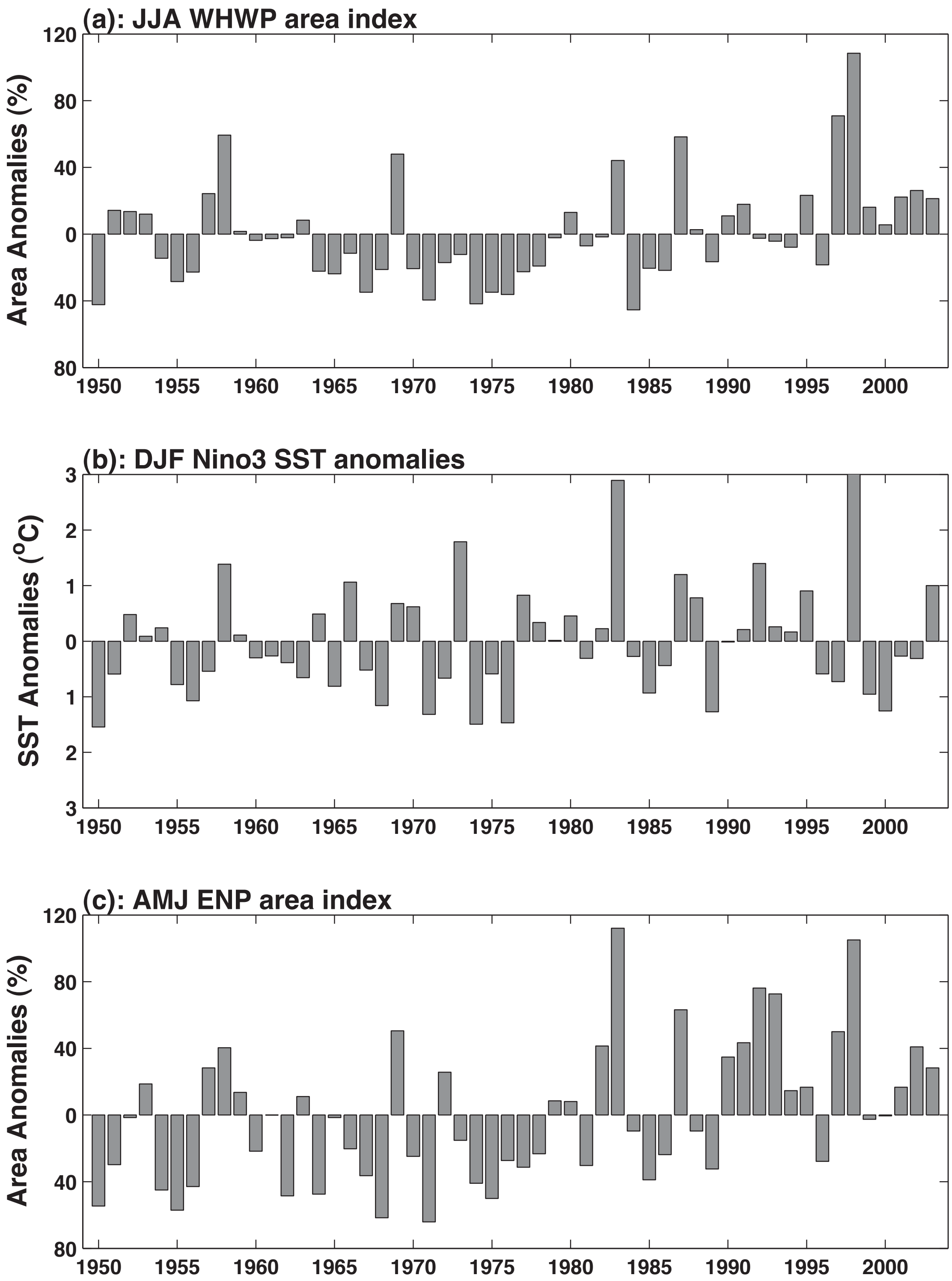

Figure 2. (a) June-July-August (JJA) Atlantic warm pool area anomaly index (%), (b) December-January-February (DJF) Nino3 SST anomalies, and (c) April-May-June (AMJ) eastern North Pacific (ENP) warm pool area anomaly index (%). The warm pool indices are calculated as the anomalies of the area of SST warmer than 28.5°C divided by the climatological (JJA and AMJ, respectively) warm pool area.

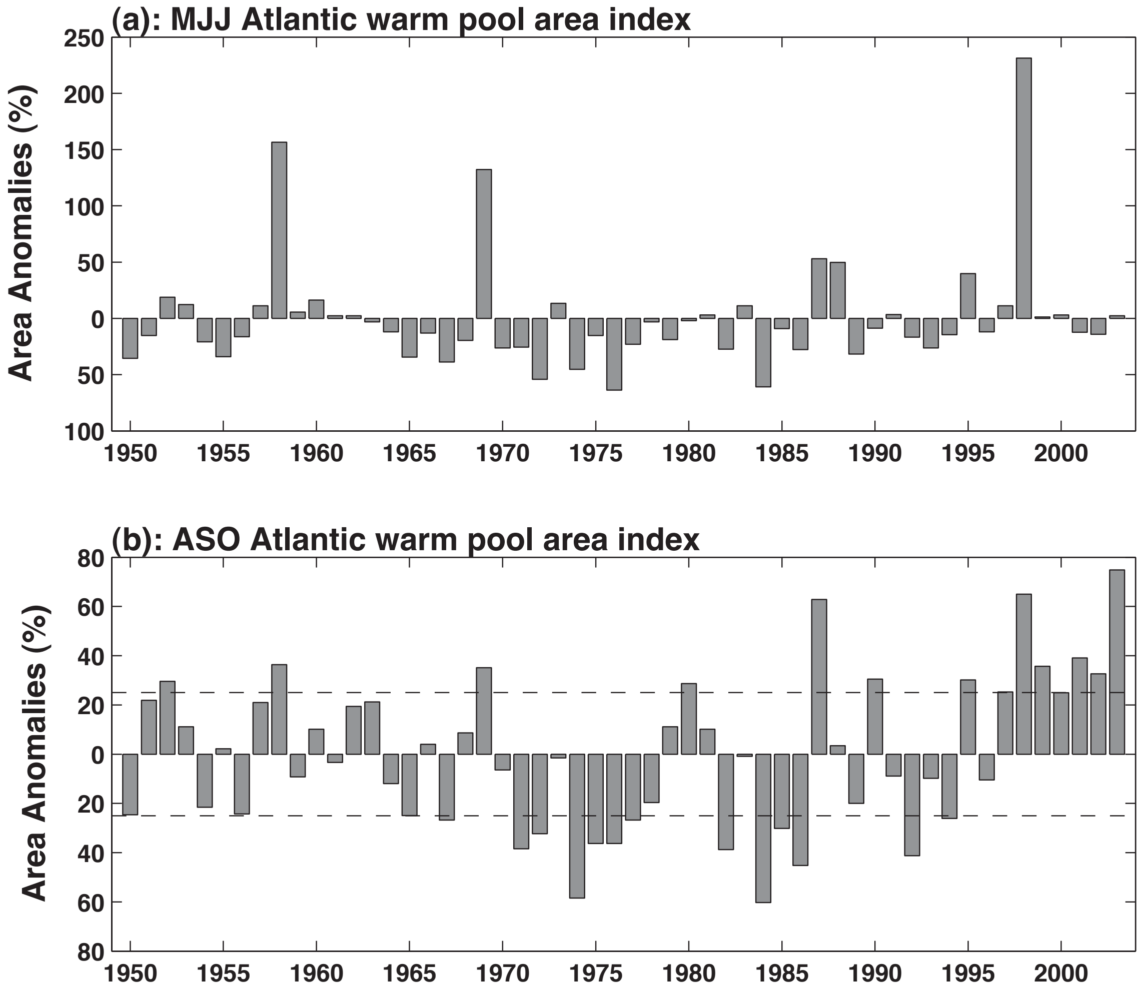

Figure 3. (a) May-June-July (MJJ) Atlantic warm pool area anomaly index (%) and (b) August-September-October (ASO) Atlantic warm pool area anomaly index (%). The indices are calculated as the anomalies of the area of SST warmer than 28.5°C divided by the climatological (MJJ and ASO, respectively) warm pool area.

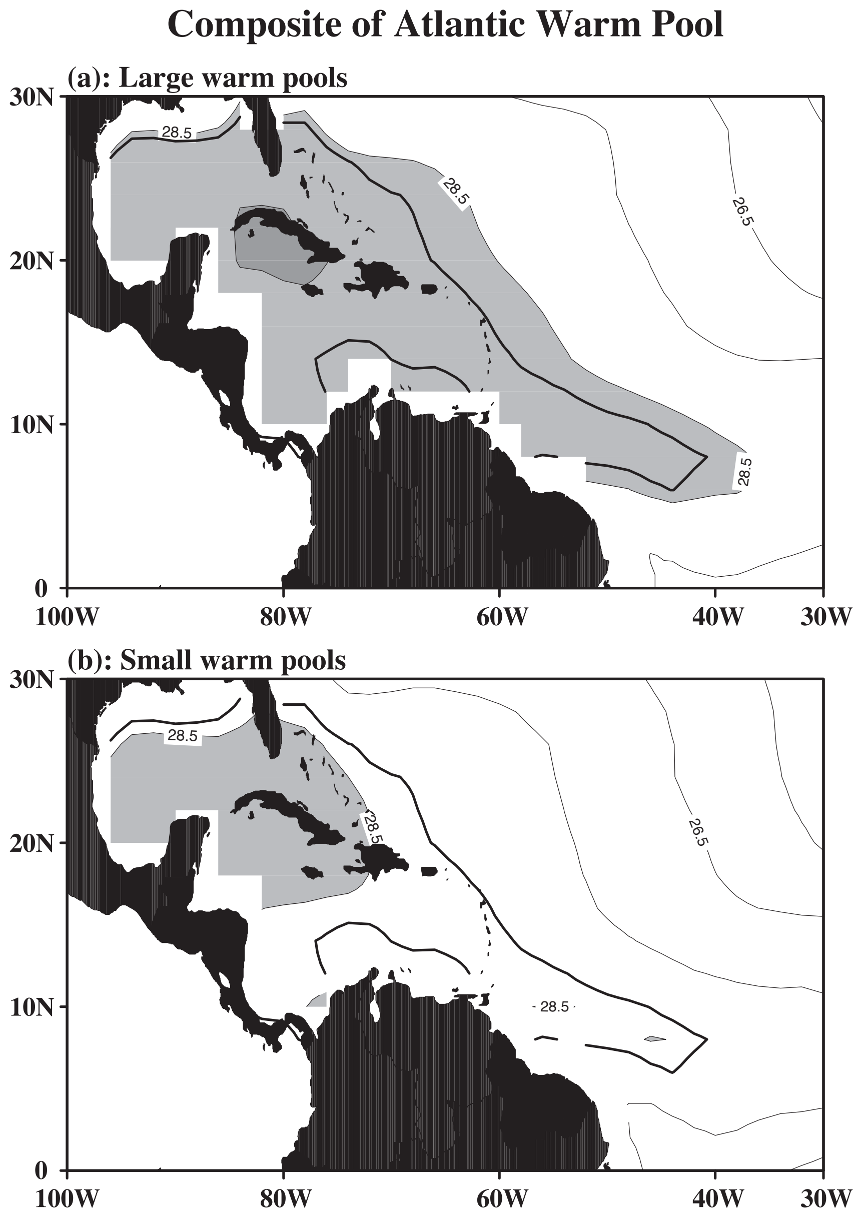

Figure 4. SST composites of (a) large Atlantic warm pools and (b) small Atlantic warm pools during August-September-October (ASO). The dark contour represents ASO climatological SST warmer than 28.5°C.

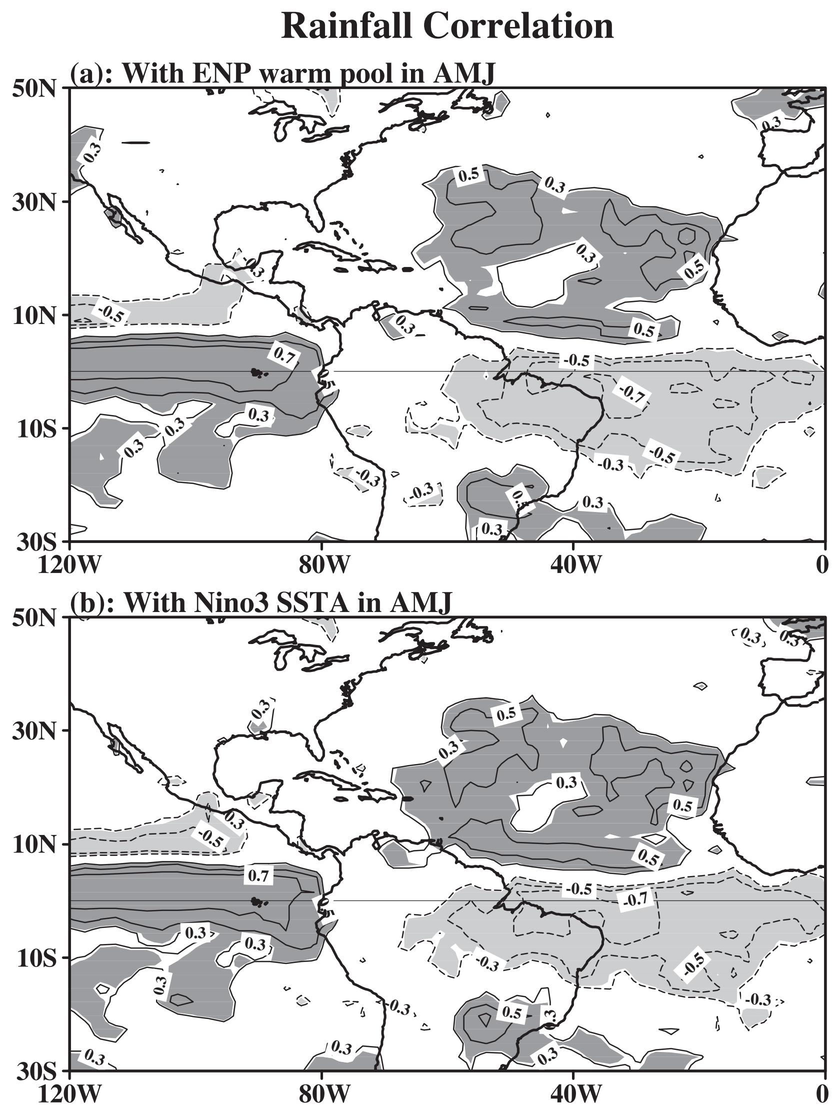

Figure 5. (a) Correlation of April-May-June (AMJ) rainfall anomalies with the AMJ eastern North Pacific (ENP) warm pool index, and (b) Correlation of AMJ rainfall anomalies with the AMJ Nino3 SST anomalies. The 90% and 95% significant levels are 0.33 and 0.39, respectively. The shadings represent correlation larger than 0.33 (dark for positive and light dark for negative).

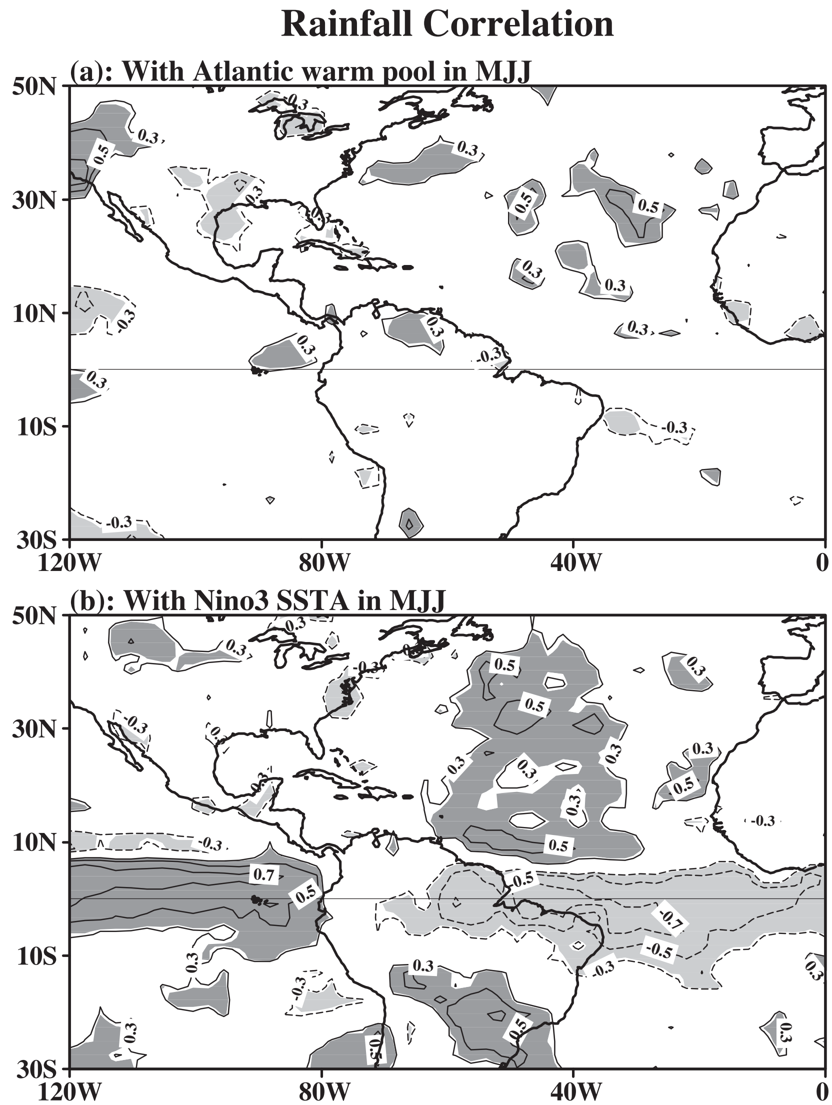

Figure 6. (a) Correlation of May-June-July (MJJ) rainfall anomalies with the MJJ Atlantic warm pool index, and (b) Correlation of MJJ rainfall anomalies with the MJJ Nino3 SST anomalies. The 90% and 95% significant levels are 0.33 and 0.39, respectively. The shadings represent correlation larger than 0.33 (dark for positive and light dark for negative).

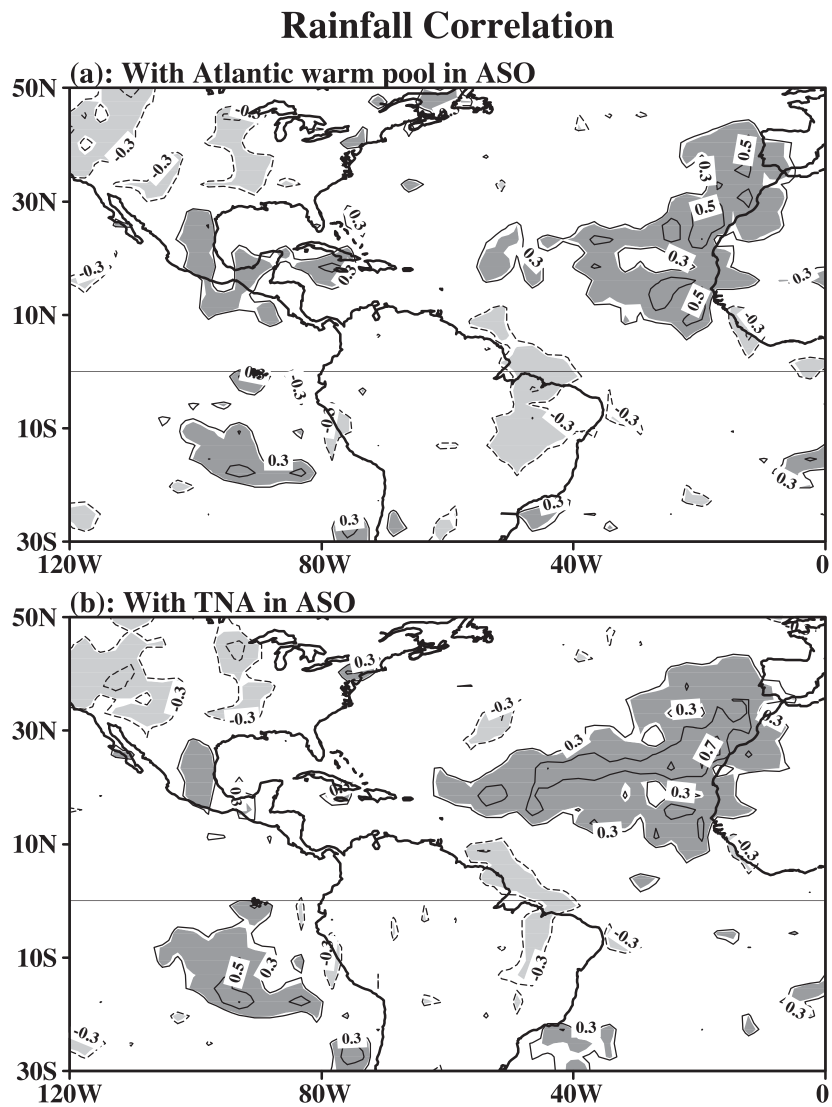

Figure 7. (a) Correlation of August-September-October (ASO) rainfall anomalies with the ASO Atlantic warm pool index, and (b) Correlation of ASO rainfall anomalies with the ASO SST anomalies in the tropical North Atlantic (TNA; 6°N-22°N, 60°W-15°W). The 90% and 95% significant levels are 0.33 and 0.39, respectively. The shadings represent correlation larger than 0.33 (dark for positive and light dark for negative).

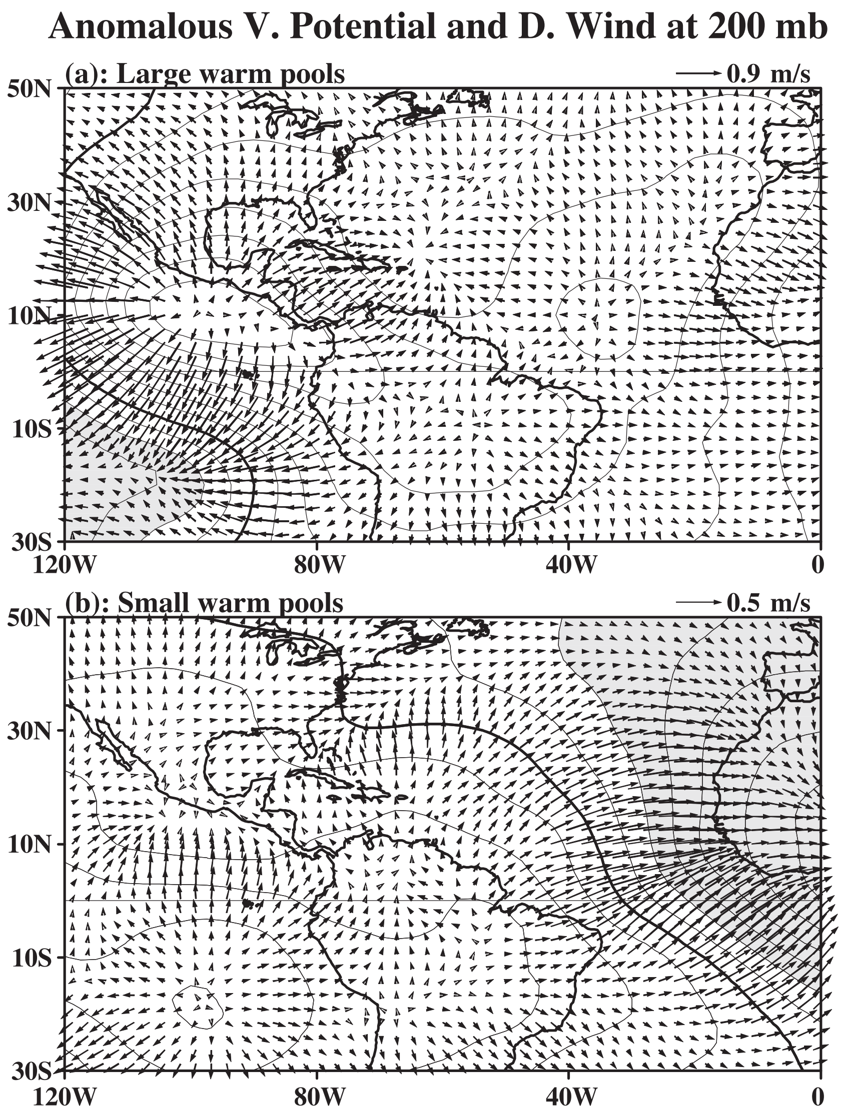

Figure 8. Composites of the 200-mb velocity potential and divergent wind anomalies during August-September-October (ASO) for (a) large Atlantic warm pools and (b) small Atlantic warm pools.

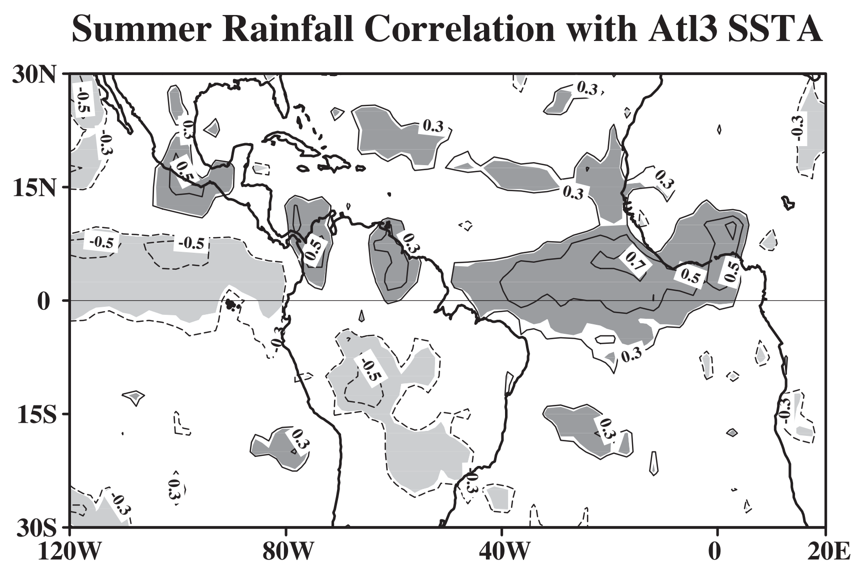

Figure 9. Correlation of June-July-August (JJA) rainfall anomalies with the Atl3 (4°S-4°N, 20°W-0°) SST anomalies. The 90% and 95% significant levels are 0.33 and 0.39, respectively. The shadings represent correlation larger than 0.33 (dark for positive and light dark for negative).

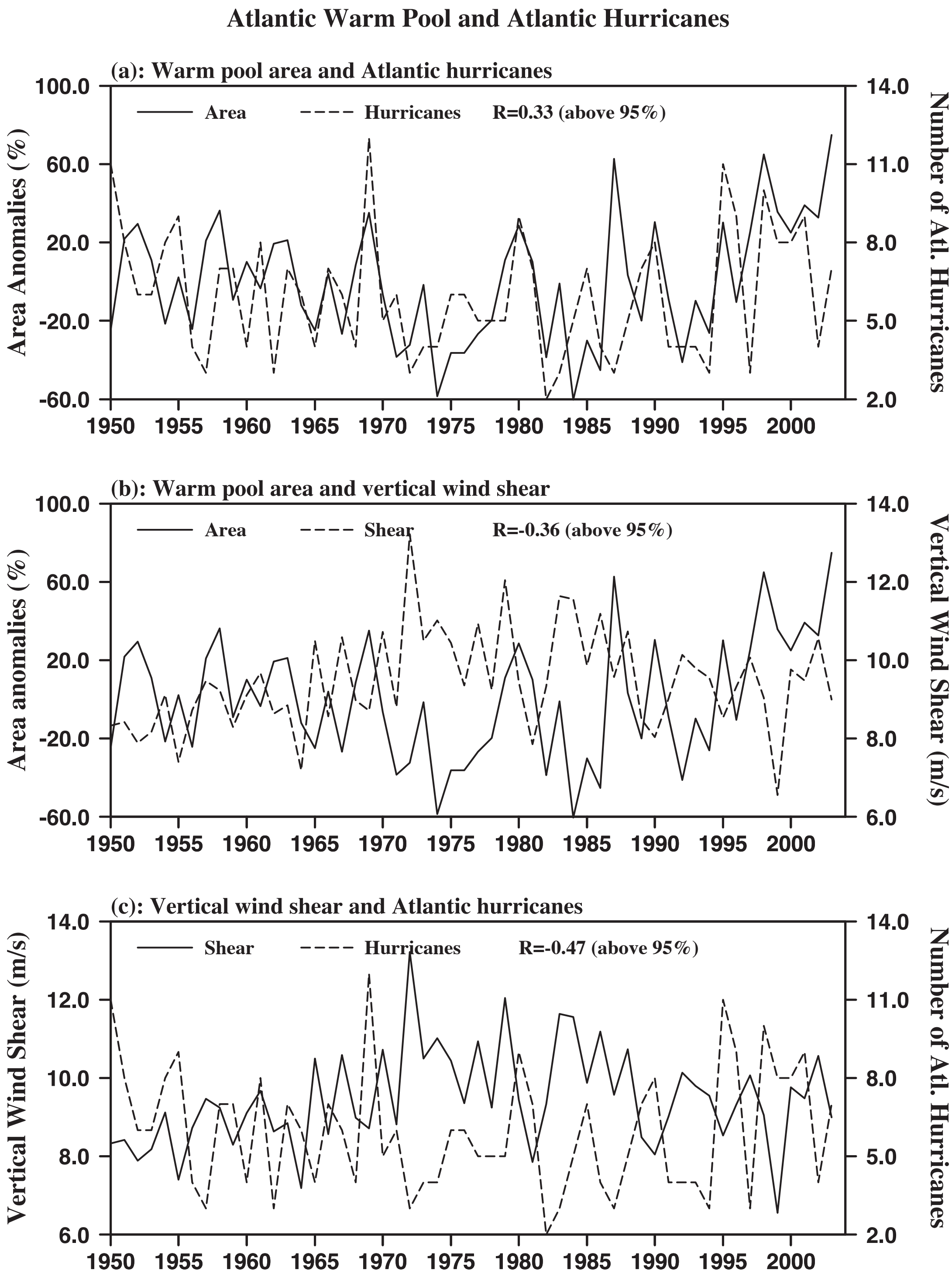

Figure 10. (a) August-September-October (ASO) Atlantic warm pool area anomalies and the total number of Atlantic hurricanes, and (b) ASO Atlantic warm pool area anomalies and the vertical wind shear between the upper (200-mb) and lower (850-mb) troposphere in the IAS region (85°W-50°W, 10°N-25°N) during ASO, and (c) the ASO IAS vertical wind shear and the total number of Atlantic hurricanes. The R represents correlation coefficient at zero lag.

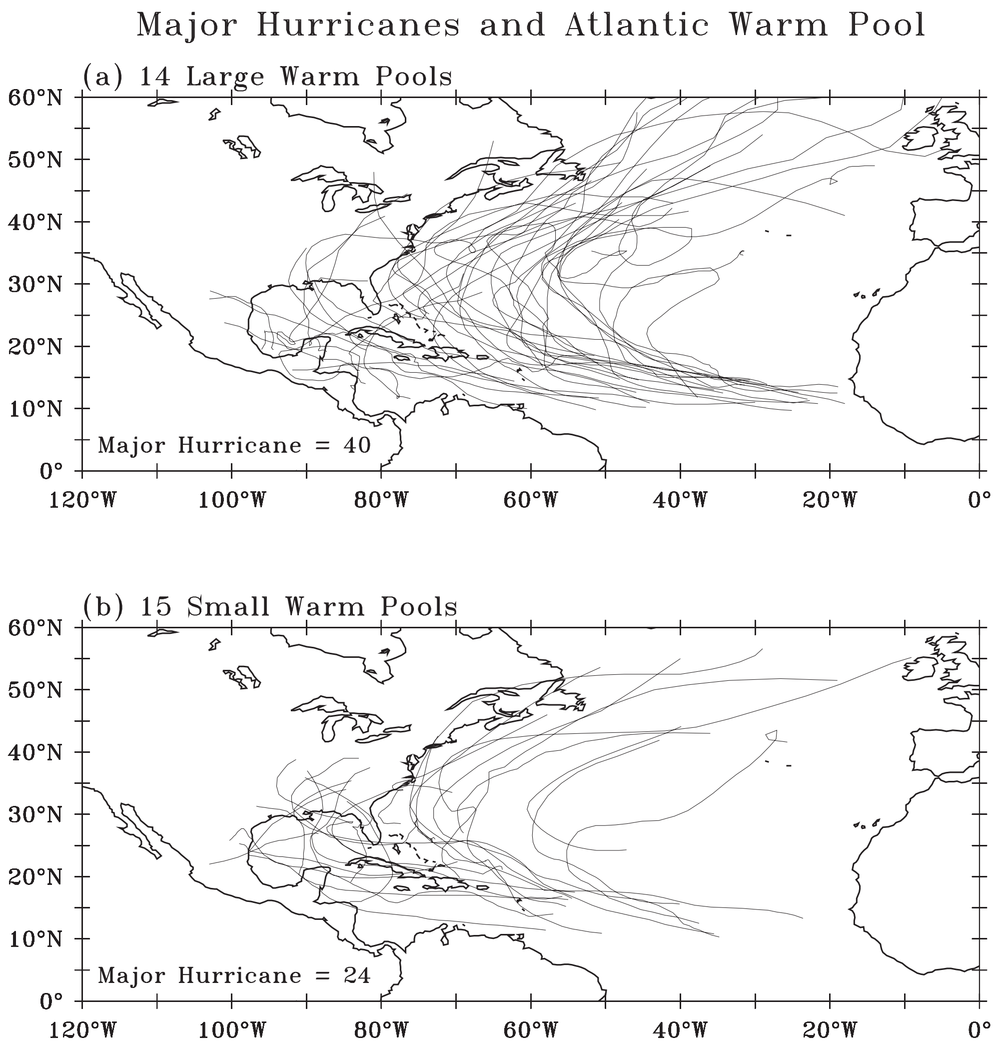

Figure 11. Atlantic major hurricane tracks for (a) 14 years of large Atlantic warm pools and (b) 15 years of small Atlantic warm pools.

Atmospheric Bridge for Linking the Pacific and Atlantic

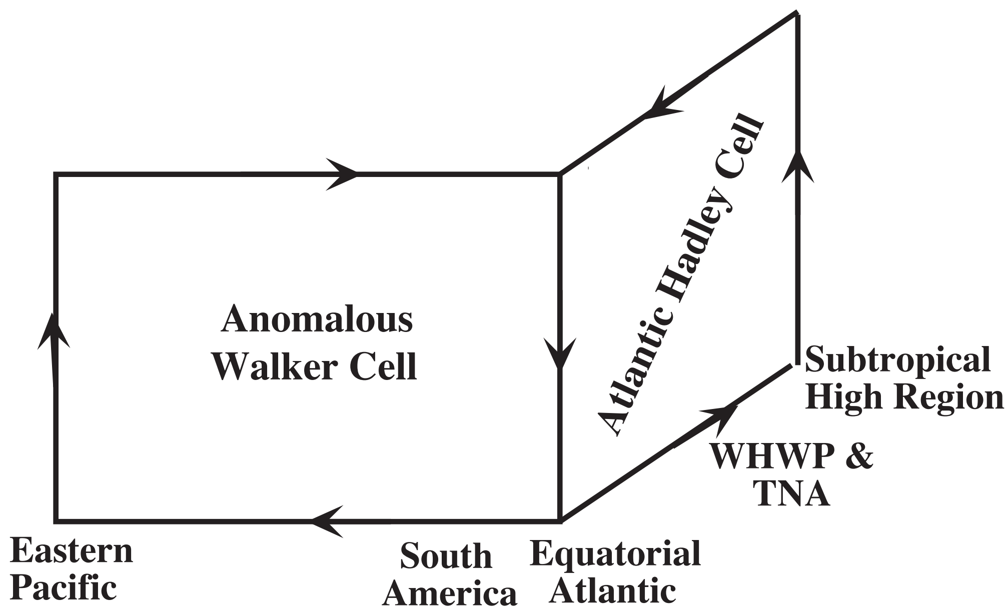

Figure 12. Schematic diagram showing linkage of the Pacific El Niño with northern South America/equatorial Atlantic, the tropical North Atlantic (TNA), and the Western Hemisphere warm pool (WHWP) by the anomalous Walker and Hadley circulations (from Wang 2002a and b). The anomalous Walker and Hadley circulations are drawn, based on the data analyzed from the NCEP-NCAR reanalysis field.